Journal of Catalysis 264 (2009) 44–53

Contents lists available at ScienceDirect

Journal of Catalysis

journal homepage: www.elsevier.com/locate/jcat

A cascade aerobic epoxidation of alkenes over Au/CeO_2 and Ti-mesoporous material by "in situ" formed peroxides

Carmela Aprile [a], Avelino Corma [a,*], Marcelo E. Domine [a], Hermenegildo Garcia [a], Chris Mitchell [b]

[a] Instituto de Tecnología Química, ITQ (UPV – CSIC), Avda. Los Naranjos S/N, 46022 Valencia, Spain
[b] Huntsman Polyurethanes, Everslaan 45, B-3078 Everberg, Belgium

ARTICLE INFO

Article history:
Received 26 January 2009
Revised 3 March 2009
Accepted 3 March 2009
Available online 23 April 2009

Keywords:
Alkene epoxidation
Aerobic oxidation
Gold catalyst
Ti-mesoporous material
Peroxide generation

ABSTRACT

The one-pot epoxidation of alkenes with O_2 is performed with nano-particulated Au/CeO_2 and Ti-MCM-41 silylated materials in the presence of a hydrocarbon and azobis-iso-butyronitrile (AIBN) as a promoter. This initiator is able to form organo-gold species that promote the formation of hydrocarbon (3-methyl-pentane, ethylbenzene, or cumene) hydroperoxides which in the presence of Ti-mesoporous material epoxidize the alkene in good yields. The epoxidation reaction of 1-octene with molecular oxygen ($P_{O_2} = 12$ bars) at 90 °C over AIBN–Au/CeO_2 + Ti-MCM-41-silylated catalytic system results in alkene conversions close to 9% (≈40% of the maximum conversion attainable) with epoxide selectivity around 90% when working with cumene as a sacrificial hydrocarbon.

1. Introduction

The epoxidation of alkenes has attracted considerable interest of the scientific community due to the versatility of epoxides as intermediates in organic synthesis [1]. At present, there are four commercial routes for the synthesis of propene oxide (PO). All are liquid processes and three of them involve the use of organic hydroperoxides (tert-butyl, ethylbenzene and cumene hydroperoxides, respectively) [2–7], and the most recent one, although not yet on stream, employs hydrogen peroxide as the oxidizing agent [8,9].

The process based on tert-butyl hydroperoxide involves a first step in which iso-butane is oxidized with air in a thermal process giving tert-butyl hydroperoxide (TBHP) and that in a second step (Scheme 1a) epoxidizes propene using a homogeneous Mo catalyst [2]. In this process, besides PO iso-butanol is also formed which is used for the production of methyl-*tert*-butyl ether (MTBE), or could also be easily converted into iso-butene which by dimerization will produce high octane gasoline [10]. In an analogous way, the other industrial processes involve the formation of ethylbenzene or cumene hydroperoxides as oxidizing agents.

It will be of interest to design a process in which the two reaction steps, i.e. the formation of the peroxide and alkene epoxidation, will occur in a cascade-type reaction where, for instance, a branched alkane will be converted into the corresponding hydroperoxide that will be immediately consumed to produce PO, following the stoichiometric reaction showed in Scheme 1b for iso-butane. In order to do this, we considered that nanoparticles of Au, supported on small crystallites (≈5 nm) of CeO_2, either as individual particles or in the form of structured mesoporous materials [11], can activate O_2 on the surface [12]. Moreover recent studies of gold reactivity with azobis-iso-butyronitrile (AIBN) have revealed that this initiator could promote catalytic oxidations by the intermediacy of R-Au organo-gold species arising from radical trapping by gold [13,14]. These organo-gold species formed on the surface of gold catalysts could promote oxygen activation via peroxo-radical species from hydrocarbons. If this is the case, it appears to us that it should be possible to form the peroxide from a branched alkane on the surface of an Au/CeO_2 catalyst when promoted by AIBN. Thus, the introduction of a second active and selective catalyst for alkene epoxidation with organic hydroperoxides (silylated Ti-MCM-41) should be able to carry out the one-pot catalyzed oxidation of alkenes in the presence of oxygen, with a branched alkane as the oxygen transfer molecule.

Previous work on gas phase propene epoxidation has been done with gold nanoparticles supported on various transition metal oxides, and silica–titania-type materials. With these catalysts H_2O_2 was "in situ" generated from H_2 and O_2 on the gold catalyst that reacted with the alkene to form the epoxide [15–21]. Thus, PO selectivities of 99% at very low alkene conversions (⩽2%) have been reported over Au/TiO_2 materials [17]. The activity of Au/TS-1 materials in this process has also been studied by Delgass and co-workers achieving 10% propene conversions with 76% selectivity

* Corresponding author. Fax: +34 963877809.
E-mail address: acorma@itq.upv.es (A. Corma).

0021-9517/$ - see front matter © 2009 Elsevier Inc. All rights reserved.
doi:10.1016/j.jcat.2009.03.010

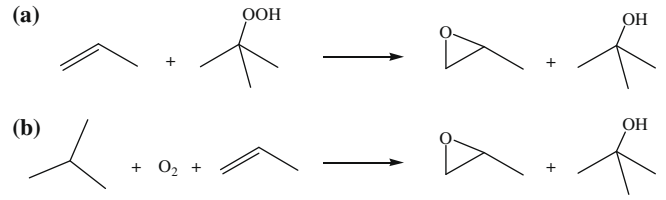

Scheme 1. Existing commercial route (a) and alternative cascade-type reaction (b) for propene epoxidation with TBHP.

to PO at 200 °C [18]. Alkene conversions of 3.2% and PO selectivity of 93.5% have been reported by Haruta research group using Au/Ti-MCM-41 materials as catalyst [19,20], while lower epoxide yields have been attained when working with Au/SBA-15 as catalysts [21]. In all the above cases, besides the low PO yields and the strong deactivation of the catalyst, one of the major drawbacks is to work with H_2 and O_2 mixtures close to the explosion threshold in order to achieve greater PO yields.

The main afore-mentioned disadvantages in propene epoxidation can be overcome by "in situ" generation of the hydroperoxide from a sacrificial hydrocarbon molecule under mild reaction conditions.

It will be shown here that by combining Au/CeO_2 and a silylated Ti-MCM-41, while using AIBN as initiator, it is possible to carry out in one pot the formation of the organic hydroperoxide of an iso-alkane (3-methyl-pentane) with O_2 and to transfer the oxygen from the hydroperoxide to the alkene (1-octene) to produce the corresponding epoxide with good selectivities. It will be also shown that the procedure can be extended to other hydrocarbons such as ethylbenzene and iso-propylbenzene (cumene).

2. Experimental

2.1. Catalysts preparation

Synthesis of meso-structured CeO_2 was performed following the procedure reported in Ref. [11]. Deposition of the gold particles on CeO_2 support was carried out by a deposition–precipitation method with $HAuCl_4 \cdot 3H_2O$ as the source of Au, following the experimental procedure detailed in [22]. Thus, a solution of 0.2 M of NaOH was added (drop by drop) to 0.6 g of $HAuCl_4 \cdot 3H_2O$ diluted in 70 ml of water (Milli-Q quality) until a pH 10 was reached. This solution of Au salt in water (pH 10) was added to a container holding 5.7 g of CeO_2 in 200 ml of water (Milli-Q quality), under continuous, vigorous agitation. The mixture so obtained was continuously stirred at room temperature for 15 to 16 h. Once the solid had been recovered by filtration, it was washed thoroughly with water and oven dried at 100 °C for approximately 12 h. The Au/CeO_2 material thus synthesized contained approximately 2.5 wt% of Au based on XRF and chemical analysis of the solid.

The Ti-MCM-41 (2.1 wt% of TiO_2) mesoporous material was prepared as reported in Refs. [23,24] starting from 3.11 g of cetyltrimethylammonium bromide (C_{16}TAB) dissolved in 20.88 g of water. Then, 5.39 g of tetramethylammonium hydroxide (TMAOH) and 0.21 g of titanium tetraethoxide (TEOT) were added to the above-mentioned solution, and the system was stirred until the titanium compound was fully dissolved. Silica (3.43 g) was then added, giving rise to a gel that was stirred at room temperature for 1 h at 250 rpm. The resulting mixture was placed into autoclaves and heated at 100 °C under autogenous pressure for 48 h. Following this time, a solid was recovered by filtration, washed thoroughly with distilled water, and dried at 60 °C during 12 h. The solid material was placed in a tubular quartz reactor where the temperature is increased from room temperature to 540 °C (under dry N_2 flow) followed by a step at 540 °C during 6 h (under dry air flow). Then the solid is cooled at room temperature. The final catalyst contains 2.1 wt% (expressed as TiO_2) based on chemical analysis. This solid has a specific surface of 1090 $m^2 \cdot g^{-1}$ with an average pore size distribution of 35 to 38 Å, and has a band in the UV–Vis spectrum centered at 220 nm.

The preparation of a silylated Ti-MCM-41 catalyst was performed as follows. Typically, 2.0 g of Ti-MCM-41 was dehydrated at 100 °C and 10^{-3} Torr for 2 h. The sample was cooled, and at room temperature a solution of 1.88 g of hexamethyldisilizane $[(CH_3)_3Si–NH–Si(CH_3)_3]$ in 30 g of toluene was added. The resulting mixture was refluxed at 120 °C for 90 min and washed with toluene. The end product was dried at 60 °C. The Ti in solid is 2.0 wt% (expressed as TiO_2) based on chemical analysis. This solid has a specific surface of 965 $m^2 \cdot g^{-1}$, and has a band in the UV–Vis spectrum centered at 220 nm. Additionally, the spectrum of ^{29}Si-MAS-RMN presents a resonance band at −10 ppm assigned to the presence of Si–C bonds.

For comparison purposes samples of Au/MCM-41 and Au/Ti-MCM-41 have also been prepared. The preparation of a purely siliceous MCM-41 mesoporous material (Si/Al molar ratio = ∞) was carried out as follows. Typically, 5.0 g of C_{16}TABr was diluted in 33.5 g of water at 40 °C. In parallel, 8.65 g of 25 wt% TMAOH solution was dispersed on 0.96 g of aerosil. Then, the last suspension was added to the initial C_{16}TABr solution at room temperature. Thus, 4.52 g of the aerosil contained in the resultant solution was hydrolyzed under stirring (350 rpm) at room temperature. The formed gel was maintained under stirring for 1 h until complete homogenization. Then, the gel (pH 13.8) was disposed into an internally Teflon-covered autoclave and heated under autogeneous pressure at 135 °C for 24 h. The obtained solid was filtered off, washed with abundant water, and oven dried at 60 °C for 12 h. Finally, the elimination of organic occluded into the solid was performed by thermal treatment (calcination) into a tubular quartz reactor where the temperature was increased from room temperature to 540 °C (under dry N_2 flow) followed by a step at 540 °C for 6 h (under dry air flow). The Si-MCM-41 sample obtained presents a specific surface area of 1000 $m^2 \cdot g^{-1}$, with an average pore size distribution of 35 to 38 Å.

Deposition of gold (Au) particles onto the surface of both Si-MCM-41 and Ti-MCM-41 mesoporous materials was performed by adaptation of the deposition–precipitation method. Typically, 1.2 g of $HAuCl_4 \cdot 3H_2O$ was diluted in 100 ml of water (Milli-Q Quality) and the pH of the obtained solution was modified with drop to drop addition of 0.2 M of NaOH solution until pH 7 to 8 was reached. Then, the mentioned Au-containing solution was added to a suspension of 6.0 g of MCM-41-type material in 200 ml of water (Milli-Q Quality) under continuous and vigorous stirring at room temperature. The mixture was maintained under stirring at room temperature for 15 to 16 h. After that, the solid was recovered by filtration, exhaustively washed with distilled water and dried in oven at 100 °C for approximately 12 h. The Au loading on the MCM-41-type supports was 4.5 and 2.3 wt% for Au/MCM-41 and Au/Ti-MCM41 catalytic samples, respectively, based on XRF measurements.

2.2. Catalyst characterization

Phase purity of the catalysts was determined by X-ray diffraction (XRD) in a Philips X'Pert MPD diffractometer equipped with a PW3050 goniometer (Cu Kα radiation, graphite monochromator), provided with a variable divergence slit and working in the fixed irradiated area mode. ^{29}Si MAS NMR spectra of MCM-41 materials were recorded at a spinning rate of 5 kHz on a Varian VXR 400S WB spectrometer. Diffuse reflectance UV–Vis (DRUV) spectra of

samples were recorded in a Cary 5 Varian spectrometer equipped with a "Praying Mantis" cell from Harrick.

Surface area, pore volume, and pore size distribution of the solid samples (200 mg) were calculated by the BET method by carrying out liquid nitrogen and argon adsorption experiments at 77 and 85 K, respectively, in a Micromeritics Flowsorb apparatus. Chemical composition was determined by atomic absorption in a Varian SpectrAA-10 Plus and elemental analysis in a Fisons EA1108CHN-S. Au content on catalysts was determined by X-ray fluorescence spectroscopy (Philips MiniPal 25 fm spectrometer). Samples for transmission electron microscopy (TEM) were ultrasonically dispersed in 2-propanol and transferred to carbon-coated copper grids. TEM micrographs were collected in a Philips CM-10 microscope operating at 100 kV. Average particle size values were obtained by measuring the diameters of about 100 particles in a representative region.

2.3. FTIR spectroscopy experiments

FTIR spectroscopic measurements of solid samples were performed with a Bio-Rad FTS 4A spectrometer equipped with a MCT detector. An IR cell allowing in situ treatments in controlled atmospheres and temperatures from 90 to 573 K was connected to a vacuum system with gas dosing facility. Oxygen-activated solid samples in the presence of AIBN were prepared ex situ as follows: an ethyl ether solution of AIBN was disposed into the reactor vessel together with the solid material. The solvent was eliminated by N_2 flow action. Afterwards, the reactor was hermetically closed, pressurized with oxygen at 12 bars, and heated at 90 °C under continuous stirring. After 1 h the reactor was rapidly frozen until 0 to 5 °C and the gas pressure decreased. The oxygen-activated sample was transferred for pellet preparation for IR measurements. Spectra of activated samples have been recorded at room temperature after background subtraction. For "in situ" IR experiments, the samples were evacuated previously followed by cumene adsorption and increase in the IR cell temperature to 90 °C.

2.4. Laser flash photolysis experiments

Photolysis of AIBN in the presence of gold salts was performed in NMR tubes. $HAuCl_4$ (6.4×10^{-2} M) was dissolved in deuterated acetonitrile (1 ml) and the radical initiator (8.0×10^{-2} M) was subsequently added. All solutions were purged with a nitrogen flow for 15 min and then irradiated using a water-refrigerated medium-pressure Hg lamp through quartz. The reaction, followed by ^{1}H NMR spectroscopy in a Varian Gemini 3000 spectrometer (300 MHz) and UV–Vis spectroscopy in a Varian Cary-5G spectrophotometer, was carried out until complete disappearance of the starting materials. For catalytic experiments, the synthesis of $H[(CH_3)_2CCN]_2AuCl_2$ organo-gold complex was performed following the same procedure mentioned above by using acetonitrile as solvent. The obtained organo-gold complex solution was then disposed into the reactor vessel and solvent was eliminated by flowing N_2 before running catalytic tests.

2.5. Catalytic experiments

Catalytic experiments were performed in a 12 ml stainless steel autoclave reactor, with an inner lining of Teflon and containing a magnetic bar. Typically, 27 mmol of 1-octene and 12 mmol of the selected hydrocarbon were placed into the reactor followed by catalyst addition, 50 mg of Au/CeO_2 sample and 100 mg of Ti-MCM-41-silylated material. When required, 15 mg (0.09 mmol) of AIBN was used as initiator. The autoclave was hermetically sealed, the lid having a connection to a pressure gauge (manometer), a second connection to allow O_2 supply, and a third outlet for samples to be taken at different time intervals. The reactor was pressurized with oxygen at 12 bars (free volume between 6.2 and 6.7 ml depending on selected hydrocarbon used), and heated at reaction temperature (90 °C), under continuous stirring. Small liquid aliquots (100 μl) were taken, filtered off, and analyzed by a 3400-Varian GC equipped with both a FID detector and a capillary column (HP-5, 30 m length), whereas identification of compounds was done by GC–MS by comparison with commercially available standards. Hydroperoxide concentration in the reaction mixture was measured using the reduction method with triphenylphosphine [25], followed by the GC analysis to determine the triphenylphosphine oxide formed that exactly corresponds to the amount of peroxide in the sample (see Supplementary material).

Alkene and hydrocarbon conversion and selectivities of products are defined as initial moles of reactant – final moles of reactant/initial moles of reactant * 100 and moles of product *i*/moles of total products * 100, respectively. Conversion of the maximum relates to the initial moles of oxygen present in the reaction media (controlling reactant) by considering that this is equivalent to the maximum amount of alkene that can be converted (100% of conversion). Hydroperoxide efficiency is defined as: moles of oxidation products from alkene/moles of hydroperoxide formed – final moles of hydroperoxide * 100. Total hydroperoxide decomposition is defined as: moles of side products derived from hydrocarbon (with an exception of hydroperoxide)/moles of hydrocarbon converted * 100.

3. Results and discussion

The metal loading and the main textural and physical properties of the catalysts used in this study are summarized in Table 1.

Experiments of aerobic oxidation of 1-octene in the presence of 3-methyl-pentane in absence of any catalyst, with and without AIBN initiator, were performed and after 3.5 h reaction time only traces of oxidation products, mainly radical allylic oxidation products, such as 1-octen-3-ol and 1-octen-3-one (see Scheme 2), and 1-octene dimerization products, were detected. Same initial experiments were also done with Au/CeO_2 or Au/MCM-41 but without AIBN. Under these reaction conditions, alkene conversion below 0.5% with epoxide selectivities lower than 75% was achieved (Fig. 1). However, when the same catalytic test with Au/CeO_2 was carried out in the presence of AIBN, the conversion increased up to 5% but the selectivity to epoxide was close to 45% after 5 h reaction time (Fig. 1). Interestingly, the same experiment but with Au-MCM-41 instead of Au/CeO_2 gave lower conversion (<2%) and selectivity to epoxide (15%), indicating the beneficial effect of combining Au/CeO_2 and AIBN for the production of the hydroperoxides (Fig. 1), since only traces of the iso-alkyl hydroperoxide were ob-

Table 1
Physical and textural properties of solid catalysts used in this work.

Catalyst	wt% Me[a,b]	Surface area (BET)/ $m^2 \cdot g^{-1}$	Metal particle size/ nm[c]
Au/CeO_2 mesostructured	2.5	185	<4.0
Au/TiO_2[d]	1.5	–	≈3.5
Au/MCM-41	4.5	860	<5.0
Au/Ti-MCM-41	2.3/ (2.0)[b]	722	15 to 16
Ti-MCM-41	2.1	1090	–
Ti-MCM-41 silylated	2.0	965	–

[a] Wt% Au measured by X-ray fluorescence spectroscopy (XRF).
[b] Wt% of Ti (as TiO_2) measured by atomic absorption spectrometry.
[c] Calculated as the medium value from transmission electron microscopy data (TEM).
[d] World Gold Council reference catalyst.

served with Au/CeO_2 if AIBN was not present. With AIBN and Au/MCM-41 as catalyst, the low amounts of initially formed hydroperoxide were non-selectively decomposed to undesired products, whereas the formation of the iso-alkyl hydroperoxide continuously increased during reaction with Au/CeO_2 instead of Au-MCM-41. However, if the hydroperoxides formed in the presence of Au/CeO_2 are not consumed rapidly to make the epoxide, they can give a large number of undesired reactions with low epoxide selectivities.

In order to improve selectivity to the epoxide, a sample of silylated Ti-MCM-41, which is very efficient to catalyze the epoxidation of alkenes with organic peroxides [23,24], was introduced together with the Au/CeO_2 catalyst and in contact with a mixture of 3-methyl-pentane (12 mmol), 1-octene (27 mmol), and O_2 (3.3 mmol) in the presence of AIBN (15 mg, 0.09 mmol). In this case, the results presented in Fig. 2 show ≈40% of the maximum conversion after 5 h reaction time, with selectivities to epoxide close to 90%. When the same experiment was carried out with Au/MCM-41 and silylated Ti-MCM-41, the conversion was lower than 20% of the maximum and the selectivity to epoxide was ≈45% after 5 h reaction time. If only Ti-MCM-41-silylated sample is used as a catalyst in the presence of AIBN, low conversions and very low epoxide selectivities are produced. Similarly, very low conversions and epoxide selectivities are observed when the Au/CeO_2 + Ti-MCM-41-silylated sample are used as catalyst but AIBN is not introduced as initiator.

It appears then that the most efficient system involves the combination of Au/CeO_2, Ti-MCM-41, O_2 and AIBN, which allows ~40% conversion and ~90% selectivity to epoxide.

The "one-pot" process described here is not exclusive for isoalkanes, but can also be applied to other oxygen transfer agents such as ethylbenzene and iso-propylbenzene (cumene). Indeed the results presented in Table 2 show conversions of, at least, 37% of the maximum after 5 h, with epoxide selectivities close to 90%. In these cases, it is possible to follow the evolution of the corresponding aryl hydroperoxide concentration with reaction time, and the selective decomposition to the corresponding alcohol when oxygen is efficiently transferred to the alkene, as well as the product formed by non-selective decomposition (mainly acetophenone in the case of cumene hydroperoxide), (see Scheme 3). As can be seen in Fig. 3, iso-propylbenzene (cumene) was selectively and continuously converted into cumene hydroperoxide (CHP

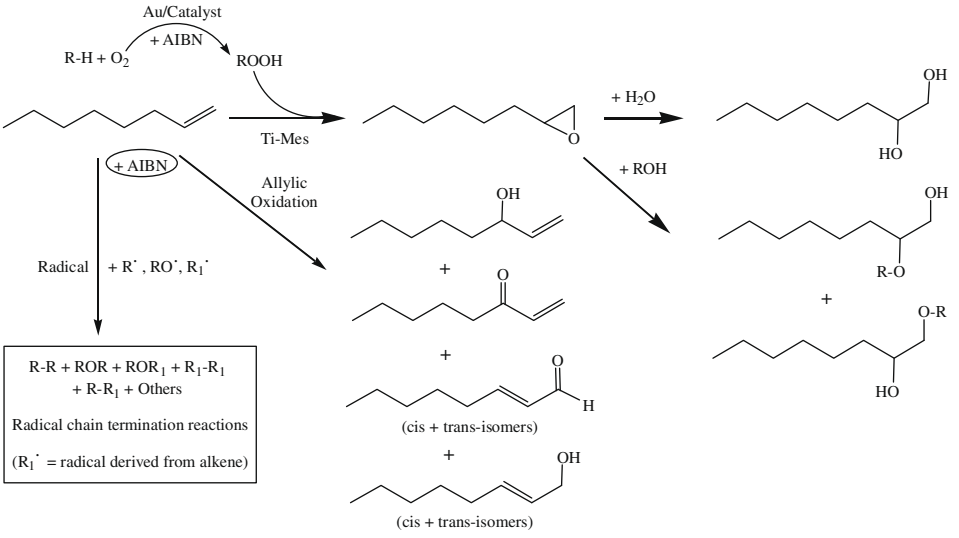

Scheme 2. Reaction network of 1-octene aerobic epoxidation.

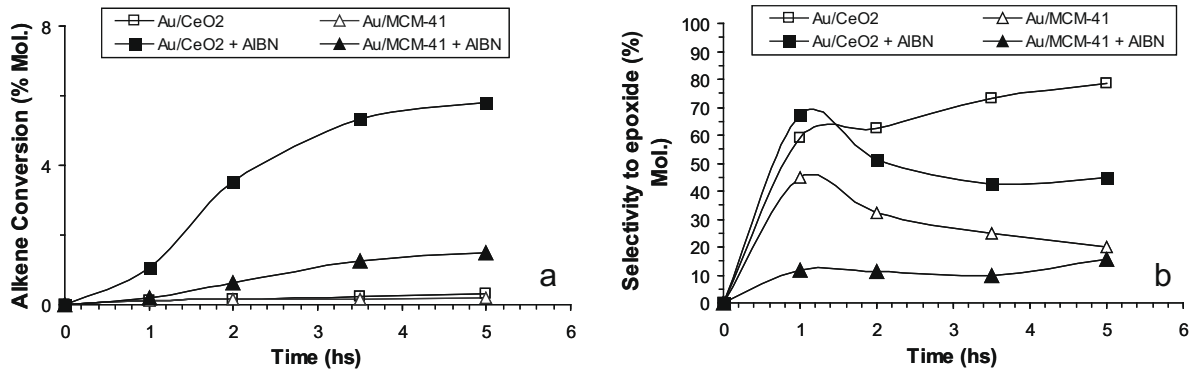

Fig. 1. Influence of AIBN addition on the 1-octene aerobic epoxidation over different gold-supported materials: (a) alkene conversion (mol.%) and (b) selectivity to epoxide (mol.%).

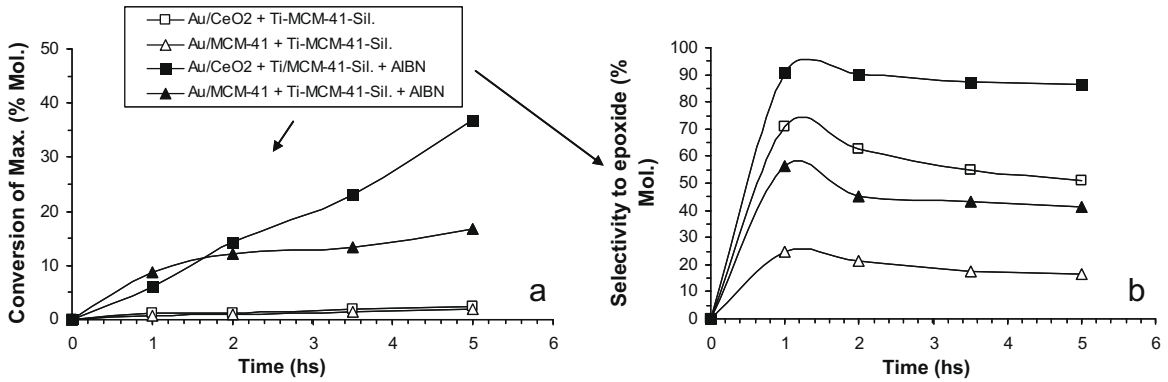

Fig. 2. Influence of the Ti-MCM-41-silylated material addition on the 1-octene aerobic epoxidation over gold-supported materials in the presence and absence of AIBN: (a) conversion of the Maximum (mol.%) and (b) selectivity to epoxide (mol.%).

Table 2
Effect of the type of hydrocarbon added during the aerobic epoxidation of 1-octene over Au/CeO_2 – Ti-MCM-41 silylated + AIBN catalytic system at 90 °C ($P_{O_2} = 12$ bars).

Hydrocarbon	Time (h)	Alkene conversion		Selectivity (mol.%)				
		(mol.%)	(% of Max.)[a]	Epoxide	Allylic oxid.		Glycol[d]	Others[e]
					C3[b]	C1[c]		
Cumene[f]	2	2.4	18.5	90.5	5.9	3.0	0.6	0.0
	5	5.3	40.9	88.4	6.1	3.5	1.4	0.6
Cumene[f,g]	3.5	3.3	–	90.0	5.5	2.7	1.3	0.5
	10	8.7	–	87.5	7.7	2.7	1.4	0.7
Ethylbenzene	2	2.0	15.4	86.7	7.3	2.8	3.0	0.2
	5	4.9	37.8	85.1	7.6	3.1	3.3	0.9
3-Methyl-pentane	2	1.9	14.3	90.1	5.8	2.7	1.0	0.4
	5	4.8	37.0	86.4	6.3	3.3	3.1	0.9
None	2	1.2	9.3	45.2	19.2	14.0	11.3	10.3
	5	3.5	27.0	42.0	22.7	10.0	10.9	14.4

[a] % of the Maximum conversion (in mols) attainable in the function of the initial amount of O_2.
[b] C3 radical allylic oxidation products = 1-octen-3-ol + 1-octen-3-one.
[c] C1 radical allylic oxidation. products = (*cis* + *trans*)-2-octenal + (*cis* + *trans*)-2-octen-1-ol.
[d] Glycol = 1,2-octanediol.
[e] Others = products derived from radical chain termination reactions.
[f] Cumene = iso-propylbenzene.
[g] Oxygen pressure was maintained at 12 bars all along the reaction.

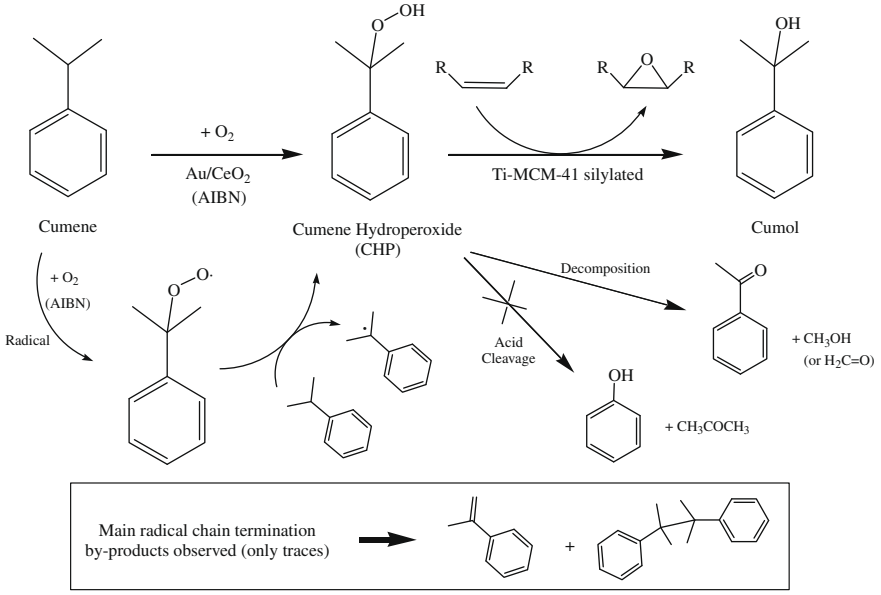

Scheme 3. Proposed reaction network for cumene hydroperoxide formation.

production ≈10% at 5 h of reaction) while high efficiency (close to 100% at 3.5 and 5 h of reaction) for the oxygen transfer reaction toward the alkene occurs. Similar behavior was observed when ethylbenzene was fed into the reactor and converted into the corresponding ethylbenzene hydroperoxide. In comparison, data obtained for 3-methyl-pentane (Fig. 4) show moderate levels of hydrocarbon conversion (<6% at 5 h of reaction) and consequently minor production of the corresponding iso-alkyl hydroperoxide although maintaining the high level of oxygen transfer efficiency (≈100% at 3.5 and 5 h of reaction). These experimental observations are in agreement with a major stabilization of radical species centered in the tertiary C directly bonded to an aromatic ring in both cumene and ethylbenzene cases.

As it is inferred from these results, the hydroperoxide generation is a key point in this "one-pot" epoxidation process. In this sense, we studied the influence of the amount of AIBN required as well as the temperature, on the hydroperoxide production when cumene is used as reactant with Au/CeO_2 sample as catalyst in the presence of molecular oxygen. Fig. 5a and b shows that the optimum amount of AIBN was around 1.5 to 1.6 wt% (≈0.07 mmol) with respect to the cumene fed into the reactor for both 90 and 120 °C temperatures, respectively. Besides this, a non-selective

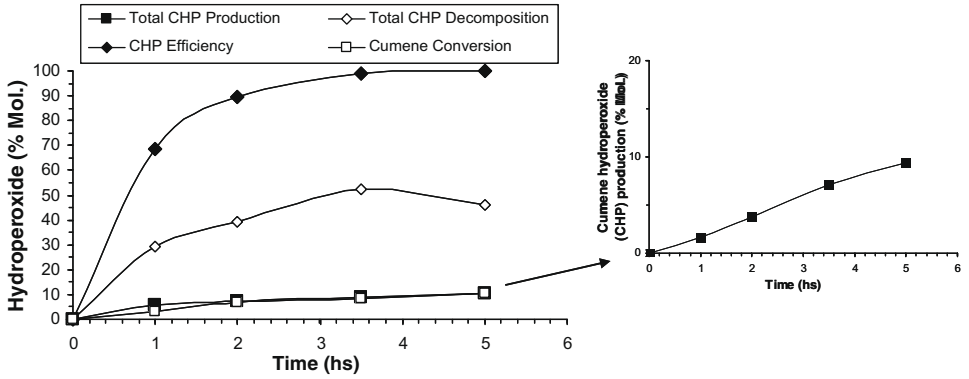

Fig. 3. Total production of cumene hydroperoxide (CHP) during the 1-octene aerobic epoxidation with Au/CeO_2 + Ti-MCM-41-silylated system in the presence of AIBN at 90 °C. The outset shows the hydroperoxide production in the 0 to 20 mol.% range.

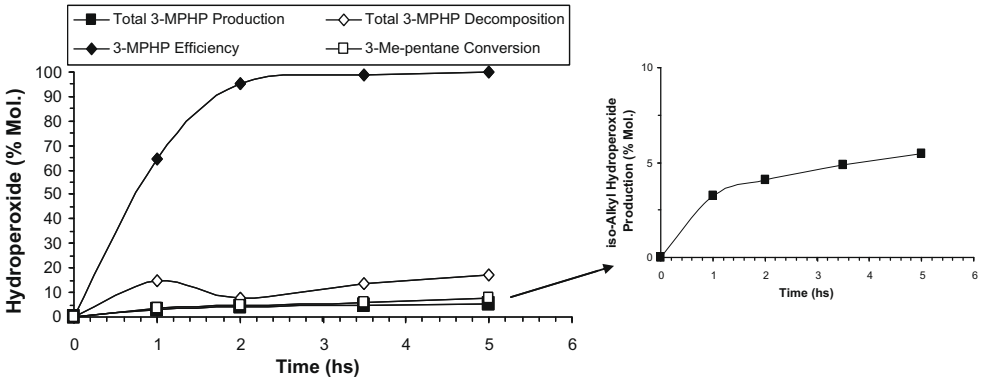

Fig. 4. Total production of 3-methylpentane hydroperoxide (3-MPHP) during the 1-octene aerobic epoxidation with Au/CeO_2 + Ti-MCM-41-silylated system in the presence of AIBN at 90 °C. The outset shows the hydroperoxide production in the 0 to 10 mol.% range.

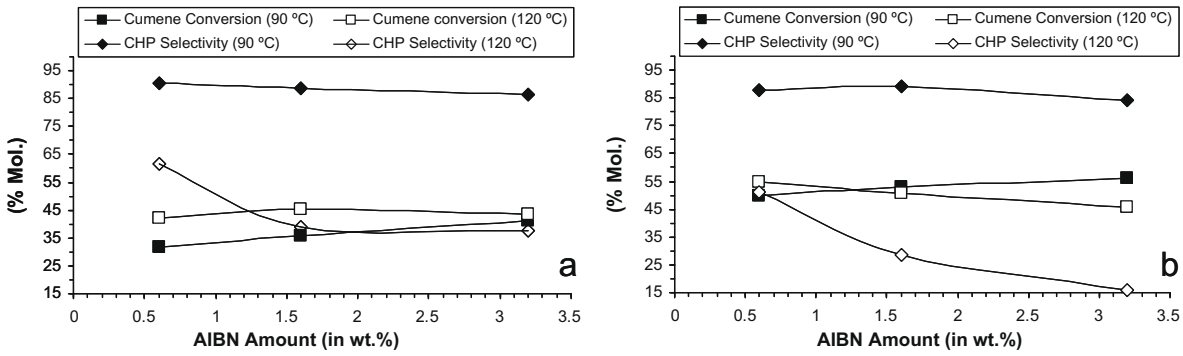

Fig. 5. Influence of AIBN amount and temperature on cumene hydroperoxide (CHP) production and selectivity with Au/CeO_2 catalyst in the presence of molecular oxygen: (a) at 2 h of reaction and (b) at 5 h of reaction.

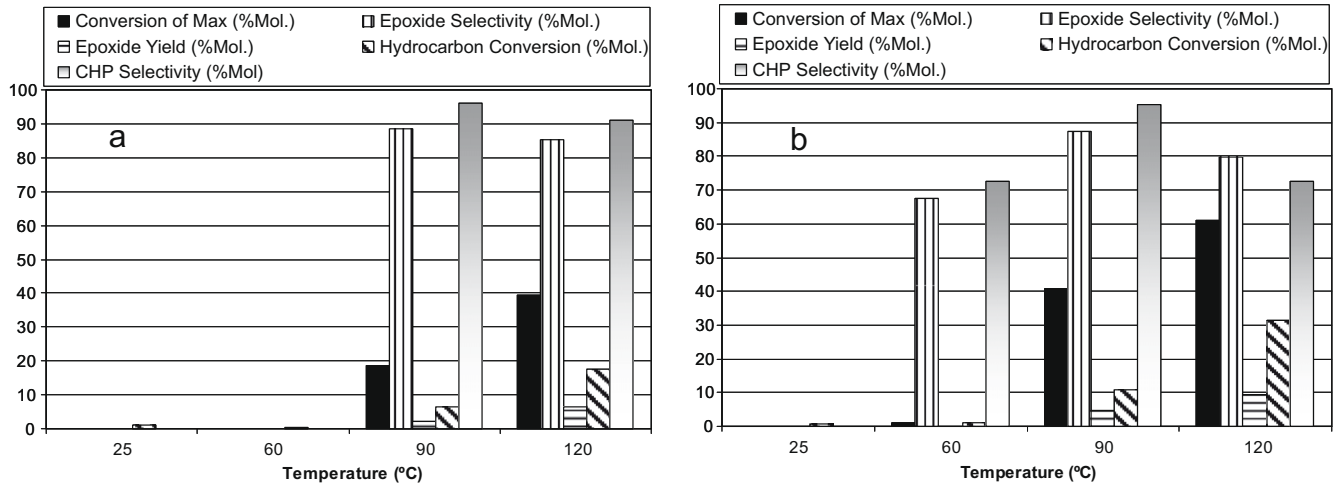

Fig. 6. Effects of temperature on the 1-octene aerobic epoxidation with Au/CeO_2 + Ti-MCM-41-silylated system in the presence of AIBN and O_2: (a) at 2 h of reaction and (b) at 5 h of reaction.

decomposition of the formed cumene hydroperoxide (CHP) was observed when the reaction temperature was increased from 90 to 120 °C (Fig. 6a and b). Thus, by working at 90 °C with the optimum amount of AIBN, the Au/CeO_2 catalyst is able to selectively produce the corresponding hydroperoxide from cumene in good yields.

The effect of temperature was also analyzed for the "one-pot" overall process by feeding cumene and 1-octene together with AIBN as initiator and Au/CeO_2 as catalyst in the presence of O_2. As can be seen in Fig. 6, at temperatures lower than 60 °C cumene was practically not converted into hydroperoxide because at this temperature initial AIBN thermal decomposition does not proceed. After 5 h of reaction, minor levels of cumene conversion with high selectivity to CHP production (≈70%, Fig. 6b) were observed at 60 °C, although the alkene epoxidation was practically not detected at this temperature. As it is mentioned above (see Table 2), good levels of cumene conversion (>10%) with high selectivity to the CHP (>90%) as well as very good levels of 1-octene epoxidation were observed when working at 90 °C (Fig. 6a and b). Additionally, cumene conversion can be increased thrice (from 10 to ≈30%, Fig. 6b) with a drastic decay in CHP selectivity (from ≈95 to ≈70%, Fig. 6b) when temperature was increased until 120 °C. In this case, alkene conversion (Conv. of Max. ≈60%) and epoxide yield (≈60%) were also enhanced with a slight decrease in epoxide selectivity from approximately 90% to 80% (Fig. 6b). All these results let us to conclude that higher temperatures favor the production of hydroperoxide as well as direct allylic alkene oxidation through a radical way instead of the catalytic ones. In this sense, a better catalytic control could be achieved by working at temperatures lower than 120 °C or in between 90 and 120 °C. This strategy should also allow avoiding the non-catalytic hydroperoxide decomposition and alkene oxidation.

The effect of the alkene/hydrocarbon molar ratio is a very important issue in this process. In this sense, we performed 1-octene aerobic epoxidation experiments over our catalytic system (at 90 °C during 5 h, $P_{O_2} = 12$ bars) in the presence of different amounts of 3-methylpentane (see Supplementary material). Results let us to conclude that an optimum alkene/hydrocarbon molar ratio (27/12) can be reached in which the epoxide yields are maximized, meaning that the formation of hydroperoxides from alkene is avoided in a large extent. In the case of cumene addition (see Supplemetary material) and due to the higher stability of cumene hydroperoxide (CHP), maximum epoxide yields are obtained at several alkene/hydrocarbon molar ratios.

It is clear that under the reaction conditions used up to now the partial pressure of O_2 decreases during reaction time. Then, we performed the alkene epoxidation at 90 °C with cumene, AIBN and Au/CeO_2 + Ti-MCM-41 silylated, wherein the O_2 pressure into the reactor was maintained constant by means of a continous controlled feed of oxygen. The results given in Table 2 show an increase in the yield of epoxide at selectivities between 88% and 90%.

Additionally, the activity of our catalytic system was compared with that of other already known gold materials, such as Au/TiO_2, with the addition of Ti-MCM-41-silylated material, and an Au/Ti-MCM-41 synthesized material under similar reaction conditions. Fig. 7 shows that the best results were obtained with the Au/CeO_2 + Ti-MCM-41-silylated catalytic system.

Evidently, AIBN is very successful in forming organo-gold species that promote oxygen activation via peroxides from the hydrocarbon present. The question now arises if other radical initiators are also able to promote the process studied here. To check this, we used benzoyl peroxide, tert-butyl-peroxybenzoate, tert-butyl and cumene hydroperoxides, and 2,2′-azobis(2-methylpropionam-

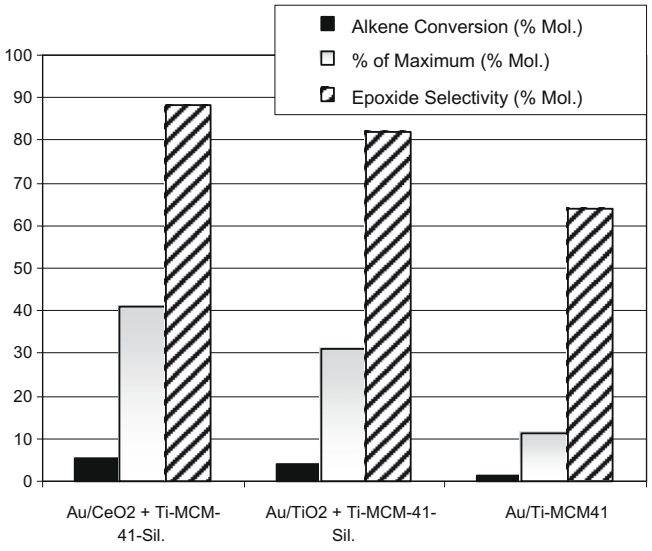

Fig. 7. Catalytic behavior of the Au/CeO_2 + Ti-MCM-41-silylated system compared with both Au/TiO_2 + Ti-MCM-41-silylated and Au/Ti-MCM-41 catalysts in the 1-octene aerobic epoxidation in the presence of AIBN (Reaction time = 5 h.).

Table 3
Effect of the type of radical initiator (0.09 mmol) added during the aerobic epoxidation of 1-octene with iso-propylbenzene (cumene) over Au/CeO_2 – Ti-MCM-41-silylated catalytic system at 90 °C during 5 h (P_{O_2} = 12 bars).

Initiator	Alkene conversion		Selectivity (mol.%)		
	(mol.%.)	(% of max.)[a]	Epoxide	Allyl. Oxid. Prod.[b]	Others[c]
AIBN	5.3	40.9	88.4	9.6	2.0
Benzoyl peroxide	0.6	4.6	74.8	23.1	2.1
CHP[d]	0.4	3.1	71.5	27.4	1.1
TBHP[e]	0.6	4.6	68.3	28.2	3.5
TBPB[f]	0.4	3.1	64.8	32.2	3.0
$ABMPA(HCl)_2$[g]	0.0	0.0	0.0	0.0	0.0
TEMPO[e]	0.0	0.0	0.0	0.0	0.0
AIBN + TEMPO[h]	1.9	14.6	84.7	15.3	0.0
AIBN + TEMPO[i]	1.5	11.5	89.3	9.7	1.0

[a] % of the Maximum conversion (in mols) attainable in the function of the initial amount of O_2.
[b] Products derived from radical allylic oxidation (1-octen-3-ol, 1-octen-3-one, *cis*- + *trans*-2-octen-1-ol, and *cis*- + *trans*-2-octenal).
[c] Products derived from epoxide ring opening (i.e. 1,2-octanediol) and 1-octenedimerization.
[d] CHP = cumene hydroperoxide.
[e] TBHP = tert-butyl hydroperoxide.
[f] TBPB = tert-butyl-peroxybenzoate.
[g] $ABMPA(HCl)_2$ = 2,2′-azobis(2-methylpropionamidine) dihydrochloride.
[h] TEMPO = 2,2,6,6-Tetramethylpiperidin-1-yloxy.
[i] TEMPO (0.09 mmol) diluted in cumene (0.1 g) added after 10 min of reaction.

idine) dihydrochloride as initiators, as well as 2,2,6,6-tetramethylpiperidin-1-yloxy (TEMPO) as radical stabilizer. The results presented in Table 3 clearly show that AIBN is by far the best promoter for the alkene epoxidation with O_2 and hydrocarbons.

3.1. Reaction mechanism

To explain the positive effect of AIBN and taking into account our previous report [13], we supposed that the first step will be the formation of an organo-gold species by the interaction of α-cyanoisopropyl radicals derived from AIBN with the surface of gold nanoparticles. Following this idea, we prepared a $H[(CH_3)_2CCN]_2AuCl_2$ organo-gold complex [AIBN–Au-complex] by reacting $AuCl_3$ with AIBN upon photochemical excitation. Catalytic tests were then performed by reacting *iso*-propylbenzene (cumene) and 1-octene with this organo-gold complex in the presence of oxygen (P_{O_2} = 12 bars) at 90 °C, and the results are given in Fig. 8. Blank experiment carried out with only AIBN reveals very low level of alkene conversion (⩽1%) with epoxide selectivities lower than 40% (Fig. 8), while practically no alkene conversion was observed with $AuCl_3$ as catalyst in the absence of AIBN. In contrast to this, the AIBN–Au-complex shows moderated catalytic activity with alkene conversion close to 4% and selectivity to epoxide around 55% at 5 h of reaction. These values can be enhanced by adding the Ti-MCM-41-silylated material to the AIBN–Au-complex reaching epoxide yields comparable to those obtained with Au/CeO_2 + Ti-MCM-41-silylated catalytic system (≈4.7%, Fig. 8). Summarizing, the formation of the epoxide in the presence of the $H[(CH_3)_2CCN]_2AuCl_2$ complex supports the hypothesis in which the intermediate is represented by "sleeping" radicals on the surface of gold when using Au/CeO_2 as catalyst.

3.2. Laser flash photolysis studies

To get some spectroscopic evidence of the interaction between α-cyanoisopropyl radical and gold nanoparticles (Aunp), we performed laser flash photolysis studies of a colloidal solution of Aunp in THF/CH_3CN in the presence and absence of AIBN. It was observed that 355-nm laser excitation of Aunp did not lead to any detectable transient in the microsecond time scale (see Supplementary data). This behavior is in agreement with the literature reporting that relaxation in excited gold nanoparticles takes place very fast in the sub nanosecond time scale [26,27] and therefore nothing should be observed when monitoring the signal in the microsecond time scale. In contrast to this, when AIBN is present in the solution a transient spectrum decaying in the sub millisecond time scale was recorded (Fig. 9). The temporal profile of the signal was coincident in all the range of wavelengths (see inset in Fig. 9) and could be fitted to a single exponential decay with a half lifetime of 65 ns. This transient spectrum is due to the interaction of radical species with gold colloid (Scheme 4). Thus, upon light excitation, decomposition of AIBN gave rise to α-cyanoisopropyl radicals and quenching of these species by gold will originate the transient species, whose spectrum is shown in Fig. 9.

It is worth noting that the formation of the above-mentioned intermediates only occurs when AIBN is used as initiator. In fact, experiments performed by reacting $AuCl_3$ with TBHP upon photochemical excitation failed to form the corresponding organo-gold complexes. Thus, this interaction of α-cyanoisopropyl radicals with gold nanoparticles is very specific and explains why none of the other initiators in Table 3 promotes the aerobic epoxidation of 1-octene via organo-gold complexes formation.

3.3. IR spectroscopy studies

Based on the above-mentioned results, the formation of organo-gold complexes seems to be a key factor for catalytic activity. However, their role in the catalytic process is not yet evidenced. For this

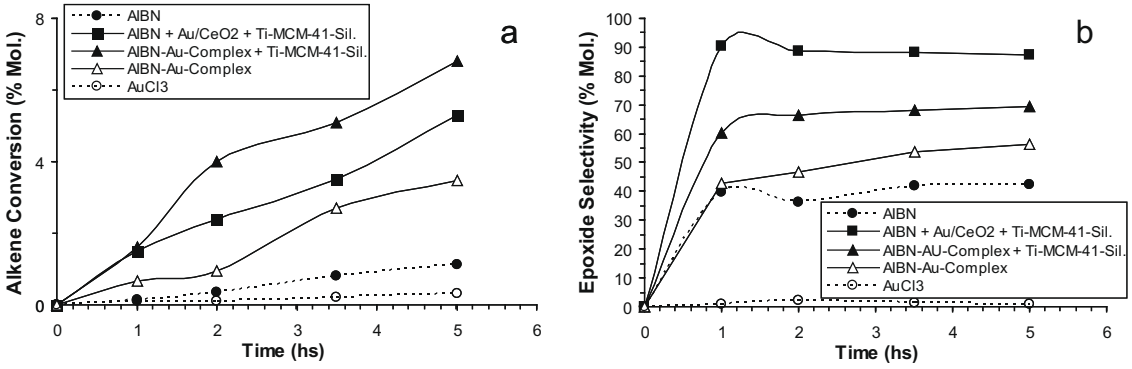

Fig. 8. [AIBN–Au-complex] catalytic behavior in 1-octene aerobic epoxidation with cumene at 90 °C. Influence of Ti-MCM-41-silylated addition and comparison with Au/CeO_2 catalyst: (a) alkene conversion (mol.%) and (b) epoxide selectivity (mol.%).

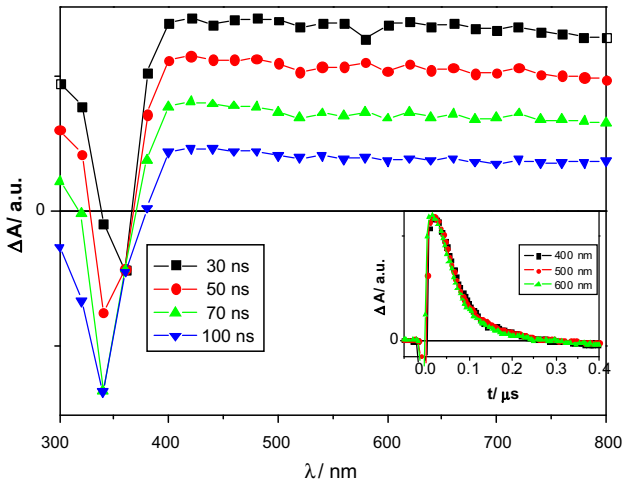

Fig. 9. Transient spectra recorded at 0.03, 0.05, 0.07 and 0.1 μs after 355 nm laser excitation of a N_2-purged THF/CH_3CN solution of gold colloid and AIBN ($3 \cdot 10^{-2}$ M). The inset shows the decays monitored at 400, 500 and 600 nm.

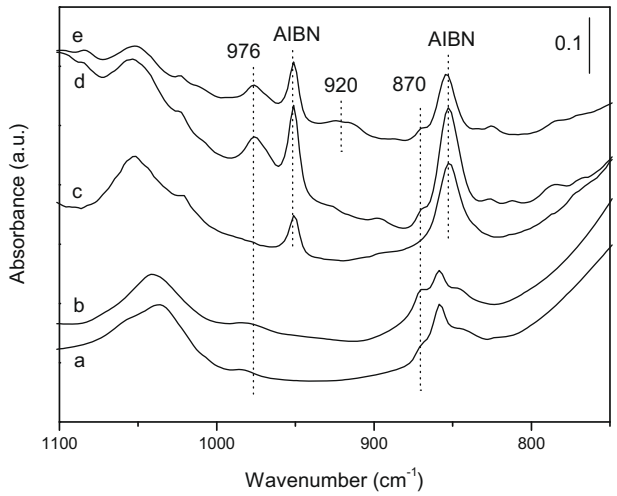

Fig. 10. FTIR spectra of oxygen-activated samples at 12 bars and 90 °C: (a) CeO_2, (b) Au/CeO_2, (c) Au/CeO_2 + AIBN (without oxygen activation), (d) CeO_2 + AIBN and (e) Au/CeO_2 + AIBN.

reason, in order to gain further insights on the reaction mechanism, in situ IR experiments have been performed.

A gold-peroxo species gives an IR band at 920 cm^{-1} [28]. In our case this band has been observed during the interaction of oxygen and Au/CeO_2 in the presence of AIBN. This species is not formed in the absence of AIBN (Fig. 10, spectra b) and consequently a promoting effect of AIBN in the formation of gold-peroxo species can be inferred. Other species such as ceria peroxo species (IR band at 870 and 976 cm^{-1}) [29,30] have also been formed on the oxygen-activated Au/CeO_2 sample in the presence of AIBN. While these ceria peroxo species are also observed in the absence of AIBN on oxygen-activated CeO_2 and Au/CeO_2 samples (Fig. 10, spectra a and b), gold-peroxo species are only formed for the presence of AIBN. Thus, the presence of AIBN is essential in the formation of an organo-gold complex, which favors oxygen activation on gold nanoparticles.

This gold-peroxo species is highly reactive toward cumene as observed from in situ IR experiments. Co-adsorption of cumene on the oxygen-activated AIBN–Au/CeO_2 sample shows a complete disappearance of the gold-peroxo species while the intensity of ceria peroxo species still remains on the catalyst surface (Fig. 11). Thus, a higher reactivity of the gold-peroxo species toward cumene can be inferred, even though the reactivity of ceria peroxo species toward cumene cannot be ruled out from our spectroscopic data. In any case, if the later process occurs it should be much slower than the one observed with gold-peroxo complexes. Indeed catalytic results show a rather low activity when using a CeO_2 catalyst with AIBN as promoter.

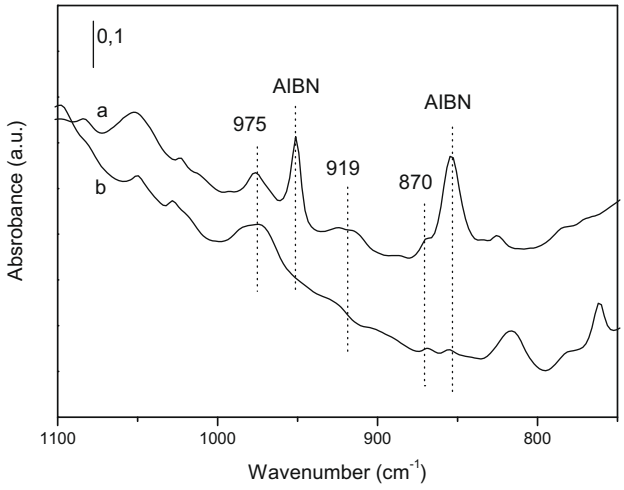

Fig. 11. FTIR spectra of oxygen-activated Au/CeO_2 + AIBN sample: (a) before and (b) after cumene adsorption at 90 °C.

3.4. Global reaction mechanism

Taking into account the catalytic experiments and all the spectroscopic evidence, we propose the mechanism illustrated in Scheme 5. The first reaction step involves the thermal AIBN decomposition into α-cyanoisopropyl radicals. These carbon-centered radicals would bind to the gold nanoparticles present on the catalyst surface, giving rise to organo-gold complexes as catalytic active species. The interaction between carbon radicals and gold nanoparticles has been proven by laser flash photolysis. Evidence for the catalytic activity of organo-gold species was obtained by performing catalytic tests with $H[(CH_3)_2CCN]_2AuCl_2$ (Fig. 8). The most likely activity of α-cyanoisopropyl-gold species would be to act as "sleeping" radicals that, in the presence of oxygen, will form of gold peroxo intermediates as evidenced by the appearance of the characteristic band at 920 cm^{-1} in the IR experiments (Fig. 10). Finally the gold-peroxo species would react with cumene through an O–O transfer generating cumene peroxides that per-

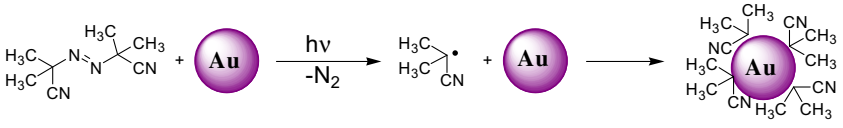

Scheme 4. Schematic representation of the interaction between α-cyanoisopropyl radical species formed from AIBN decomposition and gold nanoparticles (Aunp).

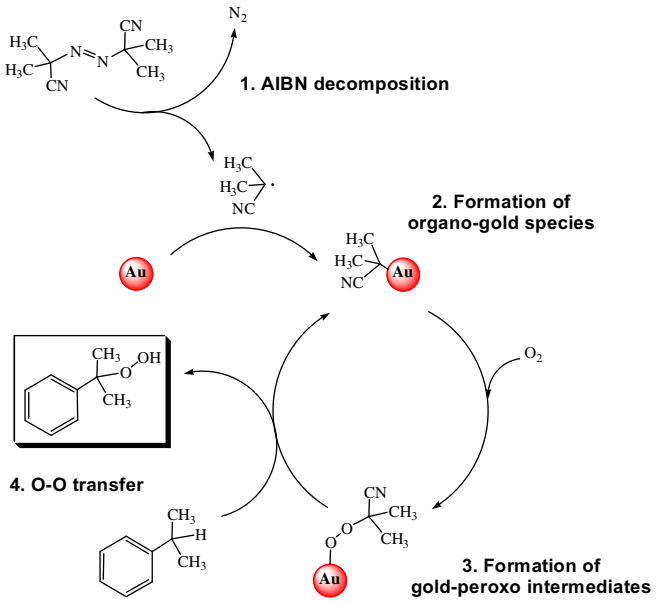

Scheme 5. Proposed mechanism for the main initiation route of hydroperoxide generation.

form the alkene epoxidation catalyzed by the silylated Ti-MCM-41 catalyst. Formation of cumene hydroperoxides is supported by the IR spectra performed in the presence of AIBN–Au/CeO_2 and cumene (Fig. 11).

4. Conclusions

It has been demonstrated here that it is possible to perform the one-pot epoxidation of alkenes (1-octene) starting with O_2 and hydrocarbons containing tertiary hydrogen, provided that the proper catalyst combination and one initiator able to form organo-gold species, which promotes the formation of the hydrocarbon hydroperoxides, are also present. Laser flash photolysis study evidenced the formation of these organo-gold species on Au/CeO_2 samples, whereas IR spectroscopic measurements let us to infer the formation of gold-peroxo species by interaction of oxygen and gold nanoparticles supported on CeO_2 nanoparticles in the presence of AIBN promoter. These gold-peroxo species are responsible for O–O transfer toward the hydrocarbon molecule adsorbed on the solid surface to produce the corresponding organic hydroperoxide which, after desorption, is used for alkene epoxidation. Thus, alkene conversion close to 40% of the maximum attainable with selectivity to epoxide around 90% can be reached in the aerobic epoxidation of 1-octene over AIBN–Au/CeO_2 + Ti-MCM-41-silylated catalytic system. The process, conveniently optimized, can be of interest for improving the efficiency of existing process for the synthesis of PO and which uses organic peroxides as oxidants, and more specifically cumene peroxide [6].

Acknowledgments

The authors gratefully thank CICYT (project MAT2006-14274-C02-01) and the Generalitat Valenciana (PROMETEO project) for financial support. We also thank J.A. Gaona and P. Concepción for help in catalytic experiments and IR spectroscopic measurements, respectively.

Appendix A. Supplementary data

Supplementary data associated with this article can be found, in the online version, at doi:10.1016/j.jcat.2009.03.010.

References

[1] Kirk-Othmer, Encyclopedia of Chemical Technology, vol. 9, fourth ed., J. Wiley & Sons, New York, 1994, p. 915.
[2] J.P. Schmidt, R.L. Bobeck, FR Patent 1 539 885, 1968.
[3] J.P. Schmidt, US Patent 3 988 353, 1976, to Oxirane Co.
[4] F. Wattimena, H.P. Wulff, GB Patent 1 249 079, 1971, to Shell Oil Co.
[5] J. Tsuji, J. Yamamoto, M. Ishino, N. Oku, Development of new propylene oxide manufacturing process, Sumitomo Kagaku (Osaka, Japan) 1 (2006) 4–10.
[6] J. Tsuji, J. Yamamoto, A. Corma, F. Rey, US Patent 6 211 388, 1998, assigned to Sumitomo Chemical Company, Ltd.
[7] M.T. Navarro, A. Corma, J.L. Jorda, F. Rey, WO 2000007710 A2, 2000.
[8] M. Taramaso, G. Perego, B. Notari, US Patent 4 410 501, 1983, to SNAM Progetti.
[9] M.G. Clerici, U. Romano, US Patent 4 824 976, 1989, to ENICHEM Sintesi S.p.A.
[10] T.S. Zak, US Patent Appl. Pub. 241 326 A1, 2006.
[11] J.Y. Chane-Ching, F. Cobo, D. Aubert, H.G. Harvey, M. Airiau, A. Corma, Chem. Eur. J. 11 (3) (2005) 979.
[12] J. Guzman, S. Carrettin, A. Corma, J. Am. Chem. Soc. 127 (10) (2005) 3286.
[13] C. Aprile, M. Boronat, B. Ferrer, A. Corma, H. Garcia, J. Am. Chem. Soc. 128 (26) (2006) 8388.
[14] M. Álvaro, C. Aprile, A. Corma, B. Ferrer, H. García, J. Catal. 245 (2007) 249.
[15] Y.A. Kalvachev, T. Hayashi, S. Tsubota, M. Haruta, Stud. Surf. Sci. Catal. 110 (1997) 965.
[16] Y.A. Kalvachev, T. Hayashi, S. Tsubota, M. Haruta, J. Catal. 186 (1) (1999) 228.
[17] A. Zwijnenburg, M. Saleh, M. Makkee, J.A. Moulijn, Catal. Today 72 (2002) 59.
[18] L. Cumaranatunge, W.N. Delgass, J. Catal. 232 (2005) 38.
[19] B.S. Uphade, Y. Yamada, T. Akita, T. Nakamura, M. Haruta, Appl. Catal. A: Gral. 215 (2001) 137.
[20] A.K. Uphade, S. Seelan, T. Akita, S. Tsubota, M. Haruta, Appl. Catal. A: Gral. 240 (2003) 243.
[21] E. Sacaliuc, A.M. Beale, B.M. Weckhuysen, T.A. Nijhuis, J. Catal. 248 (2007) 235.
[22] S. Carretin, P. Concepcion, J.M. Lopez-Nieto, V.F. Puntes, A. Corma, Angew. Chem., Int. Ed. 43 (19) (2004) 2538.
[23] A. Corma, M. Domine, J. Gaona, J.L. Jordá, M.T. Navarro, J. Pérez-Pariente, F. Rey, B. McCulloch, L. Nemeth, J. Tsuji, Chem. Commun. (1998) 2211.
[24] A. Corma, J.L. Jordá, M.T. Navarro, J. Pérez-Pariente, F. Rey, J. Tsuji, Stud. Surf. Sci. Catal. 129 (2000) 169.
[25] G.B. Shul'pin, J. Mol. Catal. A: Chem. 189 (2002) 39.
[26] C.D. Grant, A.M. Schwartzberg, Y. Yang, S. Chen, J.Z. Zhang, Chem. Phys. Lett. 383 (1, 2) (2004) 31–34.
[27] T.S. Ahmadi, S.L. Logunov, M.A. Elsayed, J. Phys. Chem. 100 (1996) 8053–8056.
[28] X. Wang, L. Andrews, J. Phys. Chem. A 105 (2001) 5812.
[29] V.V. Pushkarev, V.I. Kovalchuk, J.L. d'Itri, J. Phys. Chem. B 108 (2004) 5341.
[30] R.Q. Long, Y.P. Huang, H.L. Wan, J. Raman Spectrosc. 28 (1997) 29.